

Different temperature and pressure behavior of band edge and N-cluster emissions in GaAs_{0.973}Sb_{0.022}N_{0.005}

W. J. Wang, F. H. Su, K. Ding, and G. H. Li

State Key Laboratory for Superlattices and Microstructures, Beijing 100083, People's Republic of China

S. F. Yoon, W. J. Fan, S. Wicaksono, and B. S. Ma

School of Electrical and Electronic Engineering, Nanyang Technological University, Singapore 639798, Singapore

(Received 5 July 2006; revised manuscript received 14 September 2006; published 1 November 2006)

The photoluminescence of GaAs_{0.973}Sb_{0.022}N_{0.005} was investigated at different temperatures, pressures, and excitation powers. Both the alloy band edge and the N-cluster emissions, which show different temperature and excitation power dependences, were observed. The pressure coefficients obtained in the pressure range of 0–1.4 GPa for the band edge and N-related emissions are 67 and 45 meV/GPa, respectively. The N-cluster emissions shift to higher energy in the lower pressure range and then begin to redshift at about 8.5 GPa. This redshift is possibly caused by the increase of the *x*-valley component in the N-related states with increasing pressure. A rapid decrease of the emission intensity of the N-related band was also observed when the pressure exceeded about 8 GPa.

DOI: [10.1103/PhysRevB.74.195201](https://doi.org/10.1103/PhysRevB.74.195201)

PACS number(s): 78.55.Cr, 62.50.+p, 71.55.Eq, 71.20.Nr

I. INTRODUCTION

Nitrogen-doped III-V ternary and quaternary semiconductor materials, such as GaNAs and GaInNAs, have attracted much interest in their growth and basic physical properties for the last few decades because the incorporation of a small amount of nitrogen, acting as an isoelectronic impurity, leads to a strong modification of the host band structure, which results in a number of effects inconsistent with conventional alloys, such as a giant band gap reduction,^{1–6} a sublinear pressure dependence,^{7,8} and an increase in the electron effective mass.^{9,10} These anomalies are generally thought to be caused by the differences between the substitute nitrogen atom and the host anion in electronegativity and size. However, the explanation of the formation and evolution of the puzzling band structure that arises from the introduction of N-related states is quite controversial.

Three prevalent theoretical models have been proposed. The band anticrossing (BAC) model¹¹ indicates that a strong interaction between the conduction band and a narrow resonant band N_x leads to a splitting of the conduction band into energy levels E_+ and E_- and a reduction of the fundamental band gap. The empirical pseudopotential supercell calculations,¹² a polymorphous alloy model, show that nitrogen doping results in perturbed host states (PHS) and cluster states (CS). The PHS move down in energy and sweep the CS one by one with increasing nitrogen concentration. Another theory is the impurity band model,¹⁰ which suggests the formation of an impurity band in the band gap resulting from the convolution of different N-related states. Although these models can explain some experimental phenomena, a clear and satisfying understanding of the electronic structure of these alloys still needs further pursuing.

GaAsSbN is a potential alternative GaAs-based quaternary alloy, which has been made to produce emissions approaching 1.55 μm . The advantage of GaAsSbN arises from the fact that the band-gap energy of GaAsSbN alloy is lower than that of GaInAsN with equivalent compositions of In or

Sb for a given value of N composition. However, like GaInAsN, GaAsSbN also suffers from poor optical properties and an abnormal band structure due to the N-related defects. Therefore, the investigation of the optical properties of GaAsSbN alloy can also provide useful information about N-related impurities.

Since the application of hydrostatic pressure in studying N isoelectronic impurities in III-V semiconductor materials,¹³ it has become a powerful tool for studying the band structure of this kind of alloy. It is well known that different spectral structures can be observed in the GaAs_{1-x}N_x alloys with different N concentrations. In an ultradilute doping content ($x < 0.01\%$), the nitrogen introduces a resonant level in the conduction band.^{4,13,14} Under pressure, the resonant level shifts into the band gap and is then detected. In the alloy region ($x > 1\%$), only one emission band has been observed. The smaller pressure coefficient and nonlinear pressure behavior have frequently been observed in this case. The situation is more complicated when $0.01\% < x < 0.1\%$. Ma *et al.*⁸ have observed a series of discrete N-related below-band-gap transitions that emerge together and evolve into a broad band under pressure. Emissions from the nitrogen pair states NN_3 and NN_4 and the isolated nitrogen state N_x have also been observed by the application of pressure. Weinstein *et al.*¹⁵ have observed a pressure-induced NN_3 structure in the GaAs_{1-x}N_x alloy with $x=0.25\%$ but have not found any other structures in a sample with 0.4% nitrogen in the pressure range of 0–6.2 GPa. Kent and Zunger¹⁶ predicted that the localized-to-delocalized transition occurs at $x_c \sim 0.6\%$ for GaAs_{1-x}N_x, according to their theory. Therefore, the investigation of the behavior of the band structure and optical properties of GaNAs-related alloys at different pressures with an N concentration near the critical composition x_c is of interest.

In this work, we studied a GaAs_{1-x-y}Sb_xN_y sample with $x=0.022$ and $y=0.005$ by photoluminescence (PL) under different external environments (temperature, excitation power, and hydrostatic pressure). Both alloy band edge and

N-related emissions were observed. These emissions show different temperature, excitation power, and pressure dependences. A redshift of the N-related emission band was observed when the pressure was above 8.5 GPa, which has not been observed in other similar experiments before.

II. SAMPLE AND EXPERIMENT

The sample studied here was grown by solid-source molecular-beam epitaxy (SS-MBE) in conjunction with an N plasma source and an As and Sb valved cracker source on a semi-insulating GaAs substrate. It contains a GaAsSbN epilayer that is nominally 100 nm thick, a 100 nm undoped GaAs buffer, and a 50 nm cap layer. The as-grown sample was then annealed at 600 °C for about 5 min. The nitrogen and antimony concentrations were determined to be 0.5% and 2.2%, respectively, by x-ray diffraction measurements. The detailed growth process has been described elsewhere.¹⁷

For the hydrostatic pressure experiments, the sample was mechanically thinned to a total thickness of 20 μm , and then cut into pieces of $100 \times 100 \mu\text{m}^2$ in size. Then the sample was loaded in a diamond-anvil cell (DAC) that was used to generate pressures up to about 13 GPa. Condensed argon was used as the pressure-transmission medium. The pressure was determined from the shift of the ruby R_1 fluorescence line and was always changed at room temperature so as to ensure the best hydrostatic conditions. The PL spectra were measured at low temperatures with the DAC mounted in a He closed-cycle cryogenic refrigeration system. The actual temperature of the sample inside the DAC was determined from the intensity ratio of the R_2 line and the R_1 line of ruby.

The PL spectra were measured by a Jobin-Yvon T64000 micro-Raman system with a cooled multichannel charge coupled device (CCD). The excitation source was the 514.5 nm line of an Ar+laser with a power output tunable from 0 to 500 mW.

III. RESULTS AND DISCUSSION

A. Photoluminescence at atmospheric pressure

Figure 1(a) shows the PL spectra of the $\text{GaAs}_{0.973}\text{Sb}_{0.022}\text{N}_{0.005}$ sample under the 514.5 nm excitation with a power of about 6 mW at different temperatures. Only one peak, denoted A, can be observed at low temperature. With the increase of the temperature, peak A is quickly thermally quenched. It becomes unnoticeable at temperatures above 50 K and further disappears after the temperature reaches 90 K. At the same time, another peak, labeled B, appears at about 40 K and becomes dominant in the spectra at 60 K. An obvious difference in peak shape can be observed between peaks A and B. Peak A has a broad asymmetric shape with an exponential low-energy tail and a sharp high-energy cutoff, while peak B has a normal Gaussian-like shape. Figure 1(b) depicts the temperature dependence of the peak energy of A and B. The temperature dependence of the band gap of GaAs cited from Ref. 18 is also shown in the figure by the dotted line. The temperature dependence of band B follows the band gap of GaAs very closely, whereas band A undergoes a fast redshift with increasing temperature.

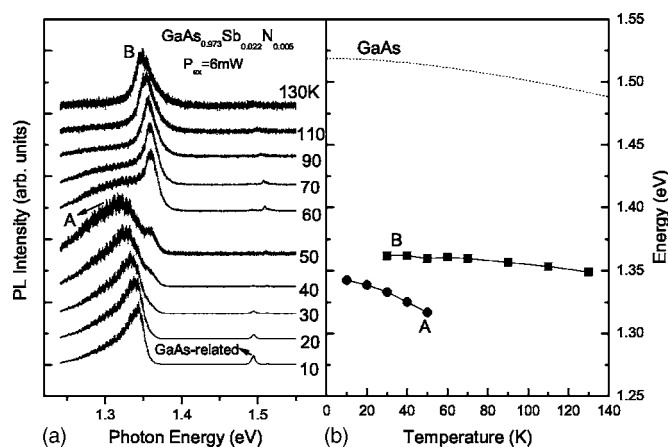


FIG. 1. (a) The PL spectra of $\text{GaAs}_{0.973}\text{Sb}_{0.022}\text{N}_{0.005}$ at different temperatures and (b) the corresponding temperature dependence of peak energy.

A similar double-peak structure has also been observed by Liang *et al.*¹⁹ in a GaInNAs/GaAs multiple quantum well with the same N concentration of $x=0.5\%$, and by Bian *et al.*²⁰ and Luo *et al.*²¹ in GaInNAs/GaAs and GaNAs/GaAs quantum wells, respectively, with higher N content ($0.77 < x < 1.5\%$). They attributed the peaks on the high-energy side to emissions from the delocalized alloy band-edge states, and assigned the peaks on the low-energy side to the N-induced impurity states or the band-tail states due to the potential fluctuation caused by the random N composition distribution. In our case, we hypothesize that peak B corresponds to the recombination of carriers at alloy band-edge states and peak A is a mixture of the emission from the band-tail states and the N-related states derived from N pairs and N clusters. With the increase of temperature, the carriers trapped by the localized states can be thermally activated into the alloy band edge. Therefore the thermal depopulation of the carriers in the localized N-related states leads to a rapid redshift of the PL maximum of band A.

Further support of our hypothesis is provided by the study of the excitation power dependences of peaks A and B. In order to monitor the changes of the two peaks together, we measured the excitation power dependences of the spectra at 55 K. Figure 2(a) shows the PL spectra measured at 55 K under different excitation powers. We note that both peaks A and B can be observed in the spectra and the relative intensity of peak B increases with increasing excitation power. The GaAs-related peaks from the cap layer also appear in the spectra, which can be used as a reference for our results. Figure 2(b) shows the excitation power dependence of the integrated intensity of peak A, peak B, and the GaAs-related peaks, where both the horizontal and vertical axes are in the logarithmic scale. When peaks A and B overlap, the integrated intensity of each peak is obtained by a deconvolution process using a symmetric and an asymmetric Gaussian function. It can be seen that the excitation power dependence of emission intensity can be well described by the relation

$$I_{PL} = CP^\alpha, \quad (1)$$

where I_{PL} is the integral intensity of the emissions, P is the excitation power, and C and α are constant. The solid lines in

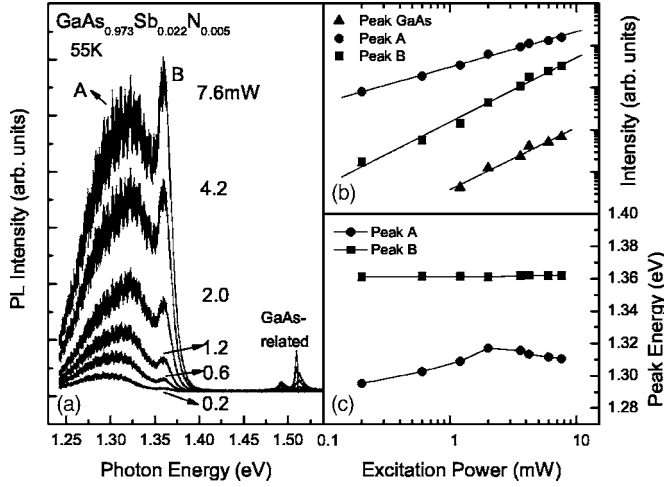


FIG. 2. (a) The PL spectra of $\text{GaAs}_{0.973}\text{Sb}_{0.022}\text{N}_{0.005}$ at 55 K under different excitation powers, (b) the power dependence of PL integral intensity, and (c) peak energy for A and B.

Fig. 2(b) are the fitted results using Eq. (1). The α obtained for peaks A, B, and GaAs are 0.84, 1.52, and 1.48, respectively. It can be seen that the slope α of B is consistent with that of the GaAs-related peaks. However, the value of α for peak A is much smaller than that of band B. This indicates that there is a similar transition mechanism between peak B and the GaAs-related peaks, but peak A has a different recombination mechanism. The weak excitation power dependence of peak A ($\alpha < 1$) is a typical behavior of localized states. Figure 2(c) depicts the variation of PL peak energy with excitation power. With increasing excitation power, peak A at first shows a significant blueshift of 22 meV, and then seems to become saturated. The PL peak energy of band B, on the other hand, remains almost unchanged. This confirms our hypothesis for peak A and peak B again. An increase of the excitation power causes a gradual filling of the localized N-related states and then results in a blueshift of the peak energy with increasing excitation density until saturation.²² In contrast, the independence of peak energy on excitation power for band B is a typical behavior of delocalized states.

B. Photoluminescence under pressure

The PL spectra of the sample under hydrostatic pressure in the range of 0–1.4 GPa are shown in Fig. 3(a) at 70 K. At first, band B dominates the spectra at ambient pressure. With the increase of pressure, band A gradually becomes the main peak and band B disappears at about 1.4 GPa. The linewidth of band A also increases continually with increasing pressure. Figure 3(b) shows the pressure dependences of the peak energies of peaks A and B. The solid lines in Fig. 3(b) are least-squares fits to the experimental data using a linear relation. The obtained pressure coefficients are 45(5) and 67(4) meV/GPa for bands A and B, respectively. The ratios for the PL integral intensity of band B to A are obtained by deconvolution of the spectra using a Gaussian function and an asymmetric Gaussian function. Its pressure dependence is presented in Fig. 3(c), in which the solid line is the theoret-

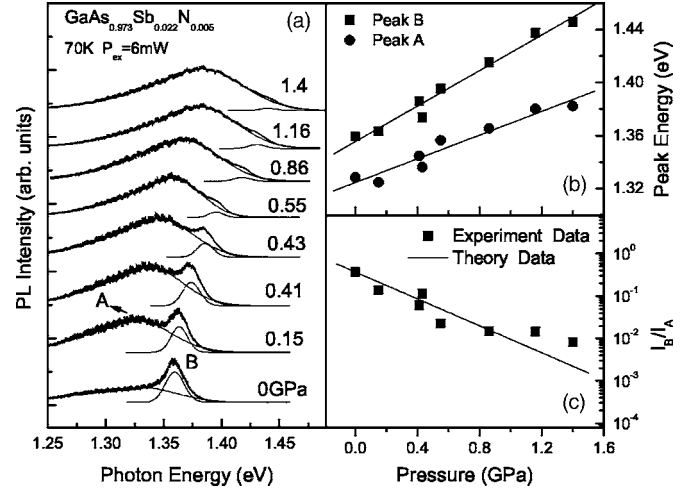


FIG. 3. (a) The PL spectra of $\text{GaAs}_{0.973}\text{Sb}_{0.022}\text{N}_{0.005}$ at 70 K in the pressure range of 0–1.4 GPa. The corresponding pressures are denoted on the right of each spectrum. The dotted curves are the deconvolved peaks. (b) The pressure dependence of peak energy of B and A, and (c) the intensity ratios of B to A are illustrated.

ical result for I_B/I_A using the exponential expression²³

$$\frac{I_B}{I_A} = I_0 \exp\left[-\frac{\alpha' p}{k_B T}\right], \quad (2)$$

where I_0 is the intensity ratio at atmospheric pressure, α' is the difference in pressure coefficient between A and B, p is pressure, k_B is Boltzmann's constant, and T is the experimental temperature. As shown in the figure, the agreement between the experimental data and the theoretical calculation is good. This indicates that the decrease of the relative intensity of band B with the increase of pressure can be well described by the decrease of the thermal occupation of the carriers in band B.

Figures 4(a) and 4(b) show the evolution of the spectra

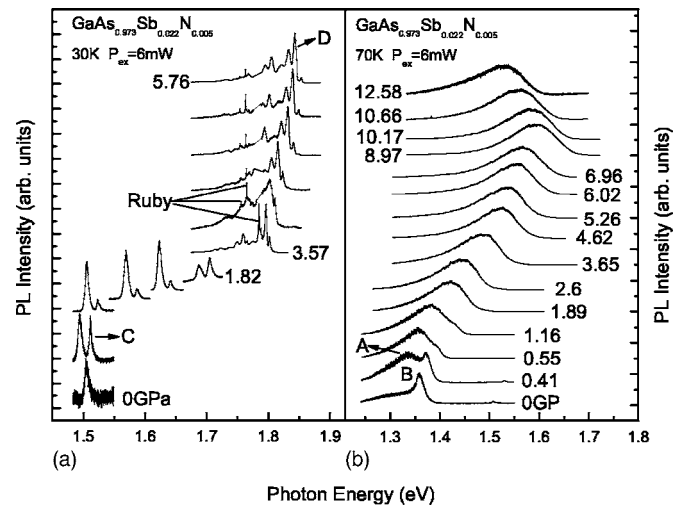


FIG. 4. The PL spectra of $\text{GaAs}_{0.973}\text{Sb}_{0.022}\text{N}_{0.005}$ under different pressures (a) in the pressure range of 1.5–1.9 eV at 30 K and (b) in 1.2–1.7 eV range at 70 K.

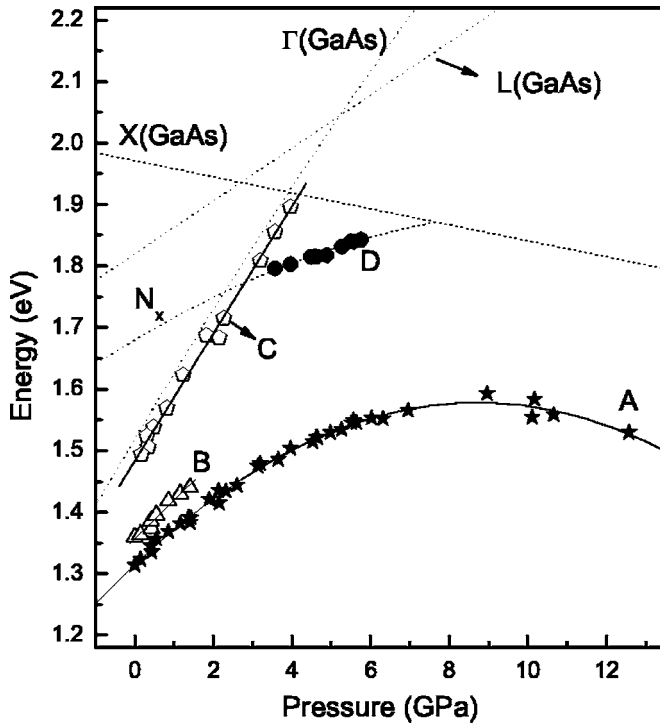


FIG. 5. The pressure dependence of peak energy for A, B, C, and D. The dotted lines are the pressure behaviors of GaAs-related valleys and N_x line at 30 K. The solid curves are the least-square fits to the experimental data.

with increasing pressure at 30 K in the energy range of 1.5–1.9 eV and at 70 K in 1.2–1.7 eV range, respectively. The most noticeable result in Fig. 4(b) is that the band A has a blueshift with increasing pressure at first. A turning point appears at about 8.5 GPa, after which band A begins to redshift. The similar pressure behavior of the band A was also observed at 30 K and is not given in this article. Another two features, labeled C and D, are observed at lower pressure. Feature C is the GaAs-related emission. It shows a very quick blueshift with the increase of pressure and then disappears at 3.96 GPa due to the Γ -X crossover in GaAs. Feature D has a multiple peak structure that is similar to the N_x line and its phonon replicas observed in Ref. 24. This feature appears in the pressure range of 3.57–5.76 GPa. The ruby lines are eliminated from the spectra of D in the figure for clarity. No other structures were observed in the measured spectra range when the pressure increased from 0 to 12.58 GPa. In order to clearly describe the pressure behavior of every peak, Fig. 5 presents the pressure dependences of the peak energies for peaks C and D at 30 K along with A and B at 70 K. The pressure dependence of the Γ , L, and X band gaps of GaAs, and of the isolated nitrogen center (N_x) obtained from the literatures^{24,25} is also indicated in the figure by the dotted lines. The solid curves are the results of the least-square fits to the experimental data using quadratic (for A) or linear relations (for B and C). The pressure coefficient of C that we acquired is about 103(3) meV/GPa, which agrees with that of GaAs-related emissions in others' works.^{13,24} The energy positions of the main peak in feature D exactly fall on the curve of N_x . Therefore we attribute

feature D to the N_x lines normally observed in the N-doped GaAs according to the spectra structure and the pressure dependence of peak position. The N_x and GaAs-related emissions may come from the GaAs cap layer into which the nitrogen was unintentionally introduced in the growth process. At high pressures, band A does not exhibit the saturation tendency reported in Ref. 11, but it begins to shift to lower energy.

It can be seen from Fig. 4 that the band A keeps one broad structure in the pressure range from 1.4 to 12.58 GPa. Under applied pressure, the spectra broadened toward lower energy. Similar broadening was also observed by Weinstein *et al.*¹⁵ in their study on the pressure behavior of GaNAs alloy with N concentrations of 0.25% and 0.4%. They attributed the broadening to the band-tail states caused by potential fluctuations. Ma *et al.*⁸ has observed one N-related emission band in the pressure range from 1.46 to 8.02 GPa for GaNAs alloy with 0.1% nitrogen and attributed this band to the N cluster states involving more than two nitrogen atoms. Comparing our work with these two reports, we propose that band A observed in our GaAsSbN sample with 0.5% nitrogen consists of emissions from both the band-tail states and the N-cluster states.

It is interesting to discuss the mechanism for the redshift of band A that we observe when the pressure is above 8.5 GPa. In the former pressure experiments mentioned above, the applied pressure was less than 8.02 and 6.2 GPa in Refs. 8 and 15, respectively. Therefore, it is unknown whether there exists a similar redshift for N-related emission in GaNAs alloy with N concentration between 0.1% and 0.4%. The applied pressure reached 12 GPa in the works of Shan *et al.* for GaInNAs alloy with N content from 0.9% to 2.3% (Ref. 11) and for GaNAs alloy with N content of 1.2% and 1.5%.⁵ However, no such redshift was observed in their experiments. The peak energies of the observed PL peaks first increased and then saturated. Since the N concentration in these samples is quite large, the observed PL structure was attributed to the alloy band-edge emission, which is different from our sample. Eremets *et al.*²⁶ reported the redshift of NN_1 emissions in N-doped GaP when the pressure is increased above about 5 GPa. With increasing pressure, the NN_1 lines approached the line of the hydrogenlike bound exciton of the X band edge in GaP and then shifted following the X band edge of GaP. We suggest that the redshift of band A in our case may also be the effect of the X valley. Mattila *et al.*²⁷ have calculated the pressure dependence of the band-edge energies in GaNAs alloy with 0.8% nitrogen based on the N-induced multiband hybridization. They indicated that the pressure behavior of the band-edge energies is determined mainly by the Γ -L interaction at lower pressure and by Γ -X interaction at higher pressure. Thus, if the band-edge states contain sufficient X character at higher pressure, it may show a redshift with increase of pressure. Band A contains the component of the fluctuation states of conduction band. Therefore, it may also have a redshift at higher pressure. Another possible reason for the redshift of band A is the increase of the X character in the N impurity centers with pressure. It is well known that the N impurity center is a deep center. Its wave function is composed of all k components of the conduction band in the Brillouin zone. At low

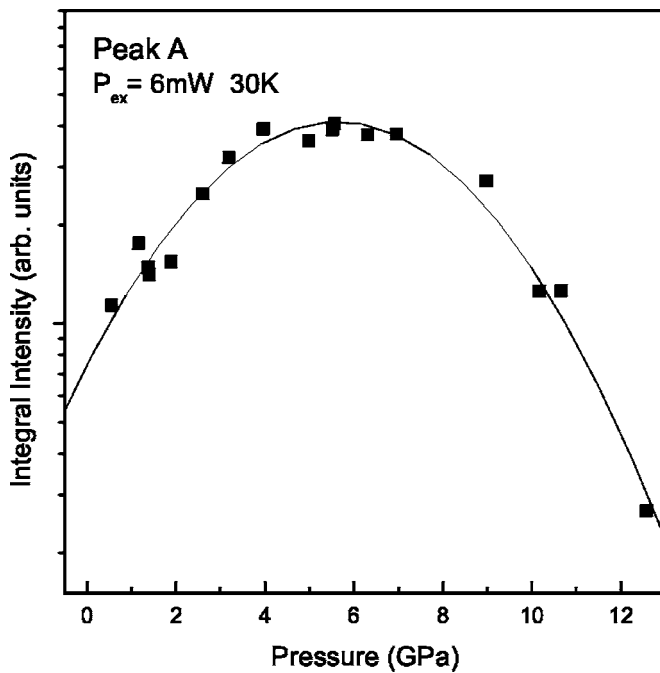


FIG. 6. The pressure dependence of PL integral intensity of A at 30 K with an excitation power of 6 mW. The solid curves are to guide the eyes.

pressure, the k components near the Γ valley dominate the wave function of the N impurity level, and band A shifts to higher energy at a relatively faster rate. With increasing pressure, the separation between the N impurity level and the Γ valley increases gradually. Thus the k component away from the Γ point increases and the shift rate of band A decreases. Beyond the Γ -X crossover, the X valley becomes the conduction band nearest to the N impurity level. The wave function of the N impurity level then involves more of the component of the down-shift X valley. If the band A approaches the X valley sufficiently, it may include enough X-component and then begin to redshift.

We have also studied the pressure dependence of the PL integral intensity of band A under a stable excitation power of 6 mW. The results are depicted in Fig. 6. It can be seen from Fig. 6 that the intensity increases with pressure at first, and then decreases rapidly when the pressure exceeds about 8 GPa. The rapid decrease of the emission intensity in the pressure range above 8 GPa is easy to understand. The X component dominates the wave function of the fluctuation states and the N-cluster states in this pressure range and increases with increasing pressure. It then causes the decrease of the transition probability of the N-related level. Consequently, the emission intensity of band A decreases rapidly. The reason for the initial increase of the intensity of band A in the lower pressure range is not known exactly. It may be ascribed to two factors: (i) the capture of the excited carriers in the conduction band by N-related levels may increase when the separation between the conduction band and the N-related level increases; (ii) the increase of light transmission due to the widened band gap of the GaAs cap layer with increasing pressure. It is worth noting that a similar initial increase of the emission intensity was also observed in a

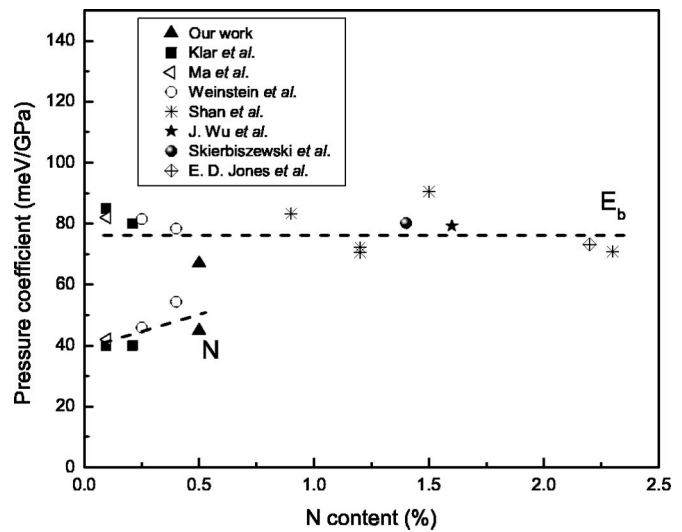


FIG. 7. The comparison of pressure coefficients in our results with those in others' work at different N contents. The dashed lines are to guide the eyes.

GaNAs/GaAs quantum well with 1.5% nitrogen.²⁴

Now we turn to discussion of the pressure coefficient of bands A and B. The pressure coefficient of band A is 45 meV/GPa in the pressure range of 0–1.4 GPa, which is in agreement with that reported by Ma *et al.*⁸ for GaNAs alloy with a nitrogen concentration of 0.1% (40 meV/GPa), Klar *et al.*²⁸ with N 0.095%, and Weinstein *et al.*¹⁵ with N 0.25% (46 meV/GPa) in the pressure range of 0–1.5 GPa. On the other hand, the pressure coefficient of band B is 67 meV/GPa, which is much smaller than the measured results of 82 meV/GPa for N=0.1% (Ref. 8) and 80 meV/GPa for N=0.21% (Ref. 28) and is also smaller than the calculated values of 78 meV/GPa for N=0.25% and 0.4%, respectively.¹⁵ Moreover, the pressure coefficients of band B are also smaller than those reported for alloy band-edge emissions of GaNAs or GaInNAs alloy with N component larger than 1%.^{5,7,11,29,30} Figure 7 shows the pressure coefficients of the alloy band-edge emission (E_b) and the N-related states (N) for different N concentrations in GaNAs or GaInNAs alloys obtained from the literature together with the results of this work. All coefficients are obtained in the low pressure range (smaller than 2 GPa). It can be seen clearly that the pressure coefficient of band B is smaller than the value for E_b in alloys with smaller N concentrations or with larger N concentrations. The reason for the smaller value obtained in this work is not well understood yet. Kent and Zunger¹⁶ predicted that a localized-to-delocalized transition will occur at $x_c \sim 0.6\%$ for GaNAs alloy. Near the critical composition, x_c , an amalgamation of states is formed, and the interaction between the localized N cluster states and the delocalized alloy band-edge states is expected to be large. Since the N concentration in our sample is 0.5%, approaching the critical component of 0.6% in GaNAs, the small pressure coefficient for alloy band-edge emission, band B, may be related to the strong interaction between alloy band-edge states and the N-related states.

IV. SUMMARY

The PL spectra of $\text{GaAs}_{0.973}\text{Sb}_{0.022}\text{N}_{0.005}$ were investigated under different temperatures, excitation powers, and pressures. Two PL peaks with very different behaviors were observed in the spectra. The temperature dependence of peak B follows the band gap of GaAs very closely, whereas peak A undergoes a fast redshift with increasing temperature. The variation of the PL intensity with the excitation power of peak B is consistent with that of GaAs-related peaks, while peak A shows a blueshift with increasing excitation level. Therefore, we attribute peak B to the recombination of alloy band-edge states and peak A to emissions from the band-tail states and the N-related centers. The pressure coefficients of peaks A and B are 45 and 67 meV/GPa, respectively, at 70 K in the pressure range of 0–1.4 GPa. The pressure coefficient of band A is in agreement with that reported previously for N-related structures, but the pressure coefficient of peak B is much smaller than that reported for alloy band-

edge emissions. This may be due to the strong interaction between alloy band-edge states and the N-related states since the N concentration in our sample is closer to the critical point of localized-to-delocalized transition in GaNAs. In the wider pressure range of 0–12.58 GPa, peak A shifts to higher energy with increasing pressure at first and then begins to redshift when the pressure exceeds about 8.5 GPa, accompanied by a rapid decrease of the emission intensity. These phenomena may be connected to the increase of the X component in the band-tail states and the N cluster states.

ACKNOWLEDGMENTS

This work was supported by the National Natural Science Foundation of China (Contract No. 60476045 and No. 10334040) and the special funds for Major State Basic Research Project of China (Contract No. G2001CB3095) at IOS.

-
- ¹M. Weyers, M. Sato, and H. Ando, *Jpn. J. Appl. Phys., Part 2* **31**, L853 (1992).
- ²S. H. Wei and A. Zunger, *Phys. Rev. Lett.* **76**, 664 (1996).
- ³W. G. Bi and C. W. Tu, *Appl. Phys. Lett.* **70**, 1608 (1997).
- ⁴J. D. Perkins, A. Mascarenhas, Y. Zhang, J. F. Geisz, D. J. Friedman, J. M. Olson, and S. R. Kurtz, *Phys. Rev. Lett.* **82**, 3312 (1999).
- ⁵W. Shan, W. Walukiewicz, J. W. Ager III, E. E. Haller, J. F. Geisz, D. J. Friedman, J. M. Olson, and Sarah R. Kurtz, *J. Appl. Phys.* **86**, 2349 (1999).
- ⁶U. Tisch, E. Finkman, and J. Salzman, *Appl. Phys. Lett.* **81**, 463 (2002).
- ⁷E. D. Jones, N. A. Modine, A. A. Allerman, S. R. Kurtz, A. F. Wright, S. T. Tozer, and X. Wei, *Phys. Rev. B* **60**, 4430 (1999).
- ⁸B. S. Ma, F. H. Su, K. Ding, G. H. Li, Y. Zhang, A. Mascarenhas, H. P. Xin, and C. W. Tu, *Phys. Rev. B* **71**, 045213 (2005).
- ⁹C. Skierbiszewski, P. Perlin, P. Wisniewski, W. Knap, T. Suski, W. Walukiewicz, W. Shan, K. M. Yu, J. W. Ager, E. E. Haller, J. F. Geisz, and J. M. Olson, *Appl. Phys. Lett.* **76**, 2409 (2000).
- ¹⁰Y. Zhang, A. Mascarenhas, H. P. Xin, and C. W. Tu, *Phys. Rev. B* **61**, 7479 (2000).
- ¹¹W. Shan, W. Walukiewicz, J. W. Ager, III, E. E. Haller, J. F. Geisz, D. J. Friedman, J. M. Olson, and S. R. Kurtz, *Phys. Rev. Lett.* **82**, 1221 (1999).
- ¹²P. R. C. Kent and Alex Zunger, *Phys. Rev. B* **64**, 115208 (2001).
- ¹³D. J. Wolford, J. A. Bradley, K. Fry, and J. Thompson, in *Proceedings of the 17th International Conference on the Physics of Semiconductors*, edited by J. D. Chadi and W. A. Harrison (Springer, New York, 1984), p. 627.
- ¹⁴X. Liu, M.-E. Pistol, and L. Samuelson, *Phys. Rev. B* **42**, 7504 (1990).
- ¹⁵B. A. Weinstein, S. R. Stambach, T. M. Ritter, J. O. Maclean, and D. J. Wallis, *Phys. Rev. B* **68**, 035336 (2003).
- ¹⁶P. R. C. Kent and Alex Zunger, *Phys. Rev. Lett.* **86**, 2613 (2001).
- ¹⁷Y. X. Dang, W. J. Fan, S. T. Ng, S. Wicaksono, S. F. Yoon, and D. H. Zhang, *J. Appl. Phys.* **98**, 026102 (2005).
- ¹⁸Y. P. Varshni, *Physica (Amsterdam)* **34**, 149 (1967).
- ¹⁹X. G. Liang, D. S. Jiang, L. F. Bian, P. Zhong, L. H. Li, and R. H. Wu, *Chin. Phys. Lett.* **19**, 1203 (2002).
- ²⁰L. F. Bian, D. S. Jiang, X. G. Liang, and S. L. Lu, *Chin. Phys. Lett.* **21**, 548 (2004).
- ²¹X. D. Luo, Z. Y. Xu, W. K. Ge, Z. Pan, L. H. Li, and Y. W. Lin, *Appl. Phys. Lett.* **79**, 958 (2001).
- ²²I. A. Buyanova, W. M. Chen, G. Pozina, J. P. Bergman, B. Monemar, H. P. Xin, and C. W. Tu, *Appl. Phys. Lett.* **75**, 501 (1999).
- ²³Guohua Li, Desheng Jiang, Hexiang Han, Zhaoping Wang, and Klaus Ploog, *Phys. Rev. B* **40**, 10430 (1989).
- ²⁴M. S. Tsang, J. N. Wang, W. K. Ge, G. H. Li, Z. L. Fang, Y. Chen, H. X. Han, L. H. Li, and Z. Pan, *Appl. Phys. Lett.* **78**, 3595 (2001).
- ²⁵G. H. Li, A. R. Goni, C. Abraham, K. Syassen, P. V. Santos, A. Cantarero, O. Brabdt, and K. Ploog, *Phys. Rev. B* **50**, 1575 (1994).
- ²⁶M. I. Eremets, O. A. Krasnovskij, V. V. Struzhkin, and A. M. Shirokov, *Semicond. Sci. Technol.* **4**, 267 (1989).
- ²⁷T. Mattila, Su-Huai Wei, and Alex Zunger, *Phys. Rev. B* **60**, R11245 (1999).
- ²⁸P. J. Klar, H. Grüning, W. Heimbrot, J. Koch, F. Höhnsdorf, and W. Stolz, *Appl. Phys. Lett.* **76**, 3439 (2000).
- ²⁹C. Skierbiszewski, P. Perlin, P. Wisniewski, T. Suski, W. Walukiewicz, W. Shan, J. W. Ager, E. E. Haller, J. F. Geisz, D. J. Friedman, J. M. Olson, and S. R. Kurtz, *Phys. Status Solidi B* **216**, 135 (1999).
- ³⁰J. Wu, W. Shan, W. Walukiewicz, K. M. Yu, J. W. Ager III, E. E. Haller, H. P. Xin, and C. W. Tu, *Phys. Rev. B* **64**, 085320 (2001).